



Formulation and characterization of a liquid crystalline hexagonal mesophase region of phosphatidylcholine, sorbitan monooleate, and tocopherol acetate for sustained delivery of leuprolide acetate



Yahira M. Báez-Santos^{a,1}, Andrew Otte^{a,1,*}, Ellina A. Mun^a, Bong-Kwan Soh^b, Chang-Geun Song^b, Young-nam Lee^b, Kinam Park^{a,c}

^a Purdue University, Weldon School of Biomedical Engineering, West Lafayette, IN 47907, USA

^b Chong Kun Dang Research Institute, 315-20, Dongbaekjukjeondaero, Giheung-gu, Youngin-si, Gyeonggi-do, 16995, Republic of Korea

^c Purdue University, Department of Industrial and Physical Pharmacy, West Lafayette, IN 47907, USA

ARTICLE INFO

Article history:

Received 22 April 2016

Received in revised form 10 June 2016

Accepted 30 June 2016

Keywords:

Drug delivery

Erosion

Liquid crystal hexagonal mesophase

PLM

Sustained-release

SAXS

Water uptake

ABSTRACT

Although liquid crystal (LC) systems have been studied before, their utility in drug delivery applications has not been explored in depth. This study examined the development of a 1-month sustained release formulation of leuprolide acetate using an *in situ*-forming LC matrix. The phase progression upon water absorption was tested through construction of ternary phase diagrams of phosphatidylcholine, sorbitan monooleate, and tocopherol acetate (TA) at increasing water content. Small angle X-ray scattering revealed the presence of lamellar and hexagonal mesophases. The physicochemical characteristics and *in vitro* drug release were evaluated as a function of the ternary component ratio and its resultant phase behavior. Formulations with increased water uptake capacity displayed greater drug release and enhanced erodability. Removal of TA resulted in increased water uptake capacity and drug release, where 8% (w/w) TA was determined as the critical concentration threshold for divergence of release profiles. In conclusion, characterization of the resultant H_{II} mesophase region provided information of the impact the individual components have on the physicochemical properties and potential drug release mechanisms. This high mitigating impact of TA on drug release indicates the use of TA as a tailoring agent, broadening the therapeutic applications of this LC system.

© 2016 Elsevier B.V. All rights reserved.

1. Introduction

Lyotropic liquid crystal (LC) structures are self-assembled structures formed due to orientational ordering of amphiphilic molecules induced by the addition of a solvent. The essential criterion for the liquid crystalline state is a certain fluidity, and at the same time, some uniformity of the average alignment of the amphiphilic molecules of the mesophase (Hiltrop, 1994). The most common LC mesophases typically are lamellar ($L\alpha$), reversed or inverted hexagonal (H_{II}), and bicontinuous cubic (V_{II}) where the latter two are gaining increased interest in drug delivery applications. This interest is due to the inherent relationship between the LC microstructure and the release rate, whereby

tuning the release of loaded molecules is attainable by changing the phase and/or composition (Negrini and Mezzenga, 2011; Phan et al., 2011). A number of well-written reviews have already been published to provide the reader with a detailed view of the structural attributes of LC mesophases and their utility for drug applications (Angelova et al., 2011; Chen et al., 2014; Drummond and Fong, 1999; Guo et al., 2010; Shah et al., 2001; Tiberg and Johnsson, 2011; Zabara and Mezzenga, 2014). Various amphiphilic materials can form LC mesophases and provide a means for controlled drug delivery, including monoolein and monovaccenin (Qiu and Caffrey, 1998), oleyl glycerate (Boyd et al., 2006), phytanyl glycerate (Boyd et al., 2006), glycerol dioleate (Johnsson et al., 2006), glyceryl monolinoleate (Nielsen et al., 1998), monoelaidin (Yagmur et al., 2008), phytantriol (Barauskas and Landh, 2003), sorbitan monooleate (Ki et al., 2014), BRIJ 97 (Phelps et al., 2011), and phospholipids (Martiel et al., 2014) among others, where many are used alone or in combination to further alter the LC structure.

* Corresponding author.

E-mail address: aotte@purdue.edu (A. Otte).

¹ These authors contributed equally.

The list of drugs that have been characterized in these systems includes but is not limited to naltrexone (Phelps et al., 2011), octreotide (Boyd et al., 2006; Tiberg et al., 2015), paclitaxel (Boyd et al., 2006), irinotecan (Boyd et al., 2006), cinnarizine (Nguyen et al., 2010), diazepam (Nguyen et al., 2010), chlorpheniramine maleate (Chang and Bodmeier, 1997a,b), diltiazem HCl (Chang and Bodmeier, 1997a,b), propranolol HCl (Chang and Bodmeier, 1997a,b), cyclosporine A (Lopes et al., 2006), somatostatin (Cervin et al., 2009), docetaxel (Cervin et al., 2010) and leuprolide acetate (Ki et al., 2014). As a result, the components used to create a LC mesophase and the potential to load a wide array of drugs from small molecules to peptides, and potentially proteins, is a major advantage of this emerging class of drug delivery systems.

LC mesophases have an internal interfacial area separated into hydrophilic and hydrophobic domains, able to entrap hydrophilic, hydrophobic, or amphiphilic molecules. The unique microstructure of LC mesophases partially controls the drug release kinetics, where the active has to diffuse through the internal microstructure to access the external environment (Boyd, 2003; Clogston and Caffrey, 2005; Shah et al., 2001). This study is focused in particular on the H_{II} mesophase, defined structurally as cylindrical micelles having negative curvature where the interface bends towards the water region (Seddon, 1990). The water component forms idealized circular rods, lined with hydrated lipid head groups, with the remaining volume filled with liquid-like hydrocarbon chains (Luzzati and Husson, 1962). While the long circular water-filled rods are often illustrated and considered as if they are open to the aqueous environment, it has been reported that these water channels are in fact closed to outside environment (Seddon, 1990; Luzzati and Husson, 1962). The release of hydrophilic drugs from the mesophase has been described as a series of dynamic events involving diffusion through water channels and permeation across the lipid bilayers (Martiel et al., 2015). However, for release of large hydrophilic molecules such as the peptide drug leuprolide acetate, random perturbation/dynamic deconstruction-reconstruction events of the reverse micelles may be required (Boyd et al., 2006).

Ki et al. (2014) have previously shown that the H_{II} -forming lyotropic LC system of phosphatidylcholine (PC), sorbitan monooleate (SMO), and tocopherol acetate (TA) is a suitable LC formulation for subcutaneous injection. The favorable pre-clinical results for the 1-month sustained-release of leuprolide acetate in rats and dogs compared with the marketed reference product, Leuplin[®] Depot injection – used for conditions such as prostate cancer, endometriosis, and central precocious puberty – highlights the therapeutic potential of this controlled-release drug delivery system (Ki et al., 2014). However, as per the inherent challenges of early phase drug development, the different *in vivo* release kinetics among the animal models impedes further correlations to humans. Therefore, it is imperative to fully characterize the liquid crystal-precursor to achieve a better understanding of its *in vivo* response. With the intent to advance the development of this LC system for the subcutaneous delivery of leuprolide acetate, we focused on characterizing the impact of the excipient components on drug release using simulated body fluid buffer (SBF – composition in Supplementary data) as a model for the physiological interstitial fluid (Marques et al., 2011). In the LC system described by Ki et al. (2014), a third component, tocopherol acetate, was added to the system as a mesophase modifier. Various mesophase modifiers have been utilized across LC systems, such as tetradecane (Sagalowicz et al., 2013), (+)-limonene (Sagalowicz et al., 2013), triolein (Sagalowicz et al., 2013), and cyclohexane (Angelico et al., 2000). Each modifier may alter the interface flexibility, the interaction with the aqueous environment, and/or the lipid chain mobility depending on the components of the system (Martiel et al.,

2014; Sagalowicz et al., 2013). Based on this, the aims of this study are: 1) to establish the different mesophases formed by the ternary components PC, SMO, and TA upon exposure to an aqueous solution; 2) to characterize the physicochemical properties of the resulting mesophases, specifically water uptake capacity and erodability; and 3) to understand the impact of the resulting mesophases and physicochemical properties on the release kinetics of the hydrophilic drug, leuprolide acetate.

Here, we demonstrate how the ternary components influence the physicochemical properties of the LC matrix and ultimately drug release, providing a means to evaluate formulation candidates in a pre-clinical setting. A link to drug release was found between the total water uptake capacity and erodability. Furthermore, H_{II} mesophases composed of the binary system of PC and SMO revealed a possible role for TA in altering drug release through modification of the mesophase's physicochemical properties. We found that formulations with low amounts of TA and higher water uptake capacities had a higher propensity towards erodability, a potential clue towards their respective *in vivo* biodegradability.

2. Materials and methods

2.1. Materials

Leuprolide acetate (LA), sorbitan monooleate (Montane[™] 80) and Tween[™] 20, tocopherol acetate (TA), and phosphatidylcholine (PC) (Lipoid S100, sourced from soybean, 96.5% phosphatidylcholine) were purchased from Polypeptide Group (San Diego, CA, USA), Seppic (Puteaux, France), DSM Nutritional Products Limited (Sisseln, Switzerland), and Lipoid GmbH (Ludwigshafen, Germany), respectively. All other chemical and reagents were of analytical grade and were purchased from Sigma-Aldrich or Fisher Scientific.

2.2. Preparation of liquid crystalline systems

The bulk phase liquid crystal precursor consists of mixing SMO, PC, and TA in their respective ratios based on the phase diagram, along with ethanol at 10% (w/w) according to the method described previously (Ki et al., 2014). In brief, SMO, PC, TA, and ethanol were weighed in a 20 mL scintillation vial and mixed overnight by continuous vortex at room temperature. The LA solution was prepared by dissolving 3.75 mg of LA in 5 μ L of DMSO. The final LC precursor formulation was designed to contain 3.75 mg of LA totaling a volume of 100 μ L.

2.3. Polarizing light microscopy

The optical properties of the LC mesophases were examined by crossed polarized light microscopy (PLM) using an Olympus BX51 (Center Valley, PA, USA) with an integrated INFINITY 1 digital camera from Lumenera (Ottawa, ON). Samples were examined under crossed polarized light after placing 20 μ L of LC precursor and 80 μ L of water as a thin film sandwiched between a microscope slide and a coverslip. Due to the anisotropic nature of the $L\alpha$ and H_{II} mesophases, sample birefringence under the crossed polarizer was used for initial qualitative phase assignment (Rosevear, 1954).

2.4. Small angle X-ray scattering (SAXS) measurements

As a means to elicit phase progression upon water absorption, ternary phase diagrams of PC, SMO, and TA were constructed at increasing water content. The synchrotron beamline 12-BM-B at the Advanced Photon Source (APS), Argonne National Laboratory, was used for SAXS measurements. Placebo samples were prepared

as described above, according to the ternary phase diagram composition ratios. Simulated body fluid (SBF) buffer was then added to the LC precursor to final a concentration of 13% (w/w), 31% (w/w), and excess, and vigorously mixed on a vortex shaker for 1–3 min to ensure homogenization. Samples were allowed to equilibrate for at least seven days prior to analysis. Samples were loaded into the backend of a syringe with a spatula and carefully injected and packed into the capillary tubes with a 1.5" 16 G needle. Samples were then held in 1.5 or 2.0 mm diameter Boron Rich capillary tubes (Charles Supper Co. Natick, MA, USA) and inserted into a block sample holder. Capillaries were positioned vertically and normal to the incident X-ray beam. SAXS data were collected at room temperature by exposing the sample to the 12.0 keV (1.0332 Å) X-ray beam. Depending on the sample's scattering intensity, exposure times of 1–5 s per frame were found optimal to maximize signal-to-noise ratio while minimizing X-ray radiation damage. X-ray scatter from the sample were recorded using a MarCCD 165 detector positioned at a sample-to-detector distance of 1.182 m. Silver behenate was used for the angular detector calibration (Huang et al., 1993).

Data reduction of the two-dimensional (2D) SAXS patterns were processed using the Nika Package (Ilavsky, 2012) from Irena to obtain one-dimensional (1D) data in the form of scattered intensity versus scattering vector, q , given by Eq. (1)

$$q = \left(\frac{4\pi}{\lambda}\right) \sin(\theta/2) \quad (1)$$

where λ is the wavelength of the incident X-rays and 2θ is the scattering angle relative to the incident of the X-ray beam. A q -range of 0.01–4.0 nm⁻¹ was used for all data collected. Bragg's law was used to analyze resulting scattering profiles based on the d -spacing and is given by Eq. (2)

$$n\lambda = 2d\sin(\theta) \quad (2)$$

where n is the scattered peak order and the lattice parameter, d , is the interplanar spacing or the distance between the centers of adjacent cylinders of the H_{II} mesophase, obtained by combining Eqs. (1) and (2) as shown in Eq. (3)

$$d = 2\pi/q \quad (3)$$

Identification of the LC mesophases was based on the relative position of the Bragg peaks on the scattering vector axis. SAXS patterns with q -spacing ratios of 1:√3:√4:√7, etc. correspond to H_{II} mesophase, whereas ratios of 1:2:3:4, etc. correspond to $L\alpha$ mesophase (Hyde et al., 1997).

2.5. Physicochemical characterization

2.5.1. Determination of water content – depot and H_{II} boundary conditions

A total of 100 μL of LC precursor was injected onto 3 mL of SBF and water uptake for the resultant LC matrix was determined by Karl Fischer titration using a Mettler Toledo (Columbus, OH, USA) V20 Titrator. Anhydrous methanol was used as the solvent and Hydranal®-Composite 5K was used as the titrant. Triplicate samples for each time point were prepared, and water content was determined at 1, 6, and 72 h, and 7, 10, 14, and 21 days. For each time point measurement, the LC matrix was removed from the SBF and initially placed on weighing paper to remove any excess SBF that was transferred during the removal from the vial. Next, the LC matrix was placed on fresh weighing paper, weighed, and then analyzed via Karl Fischer titration.

For the H_{II} + excess water boundary condition, samples were prepared as described above except that 200 μL of LC precursor was injected into 3 mL of SBF. After injection, the mixtures were

vortexed for 30 s on a vortex shaker. The samples were then vortexed again for 30 s on day 2, 3, and 4. On day 5, the samples were centrifuged, and excess water was removed. The LC matrix was then removed from the vial, initially placed on weighing paper to remove any excess SBF that was not removed during the centrifugation. Next, the LC matrix was placed on fresh weighing paper, weighed, and then analyzed via Karl Fischer titration.

2.5.2. Erosion assay

In a 20 mL scintillation vial, a total of 100 μL of LC precursor was injected onto 3 mL of SBF and allowed to swell for 72 h at room temperature. After swelling, 7 mL of SBF containing 1.42% (v/v) Tween 20 was added to obtain a final concentration of 1% (v/v) Tween 20 and a final volume of 10 mL. Samples were incubated at 37 °C and shaking at 200 rpm. Time points of 100 μL were taken, placed in UV/vis 96-well microplates, and the absorbance of TA and SMO from the dispersed LC precursor was recorded at the peak maximum of 280 nm. For each LC precursor, standard curves of erosion were built by allowing the LC precursor to reach 100% erosion under the same conditions, followed by serial dilutions into SBF containing 1% (v/v) Tween 20. Blank control samples (1% (v/v) Tween 20 SBF solution) were used for background corrections. The absorbance of the samples was at least 2-fold the signal of the background controls. Each experiment was performed in triplicate.

2.5.3. In vitro drug release profile of leuprolide acetate

To evaluate the 1-month *in vitro* release of LA from LC precursor formulations, 100 μL of LC precursor loaded with LA (3.75 mg) was injected into a Pur-A-Lyzer™ Mini 12000 dialysis tube to prevent the formed LC matrix from floating and breaking on the walls of the scintillation vials. The dialysis tube was then placed into 10 mL of SBF (0.02% w/v Sodium Azide) pre-equilibrated to 37 °C. For drug release from a partially formed LC matrix, formulations were prepared at 13% (w/w) aqueous content and mixed overnight. The resulting 100 μL dose contained 3.25 mg of LA. Drug release was then analyzed for 28 days under 37 °C and constant shaking of 100 rpm. Aliquots of 1 mL were taken at 1, 6, and 24 h, and day 2, 3, 4, 5, 7, 13, 15, 17, 20, 22, 24, and 28, followed by replacement of media with 1 mL of SBF. Samples were filtered using a 0.45 μm Captiva syringe filter (Agilent Technologies) prior to analysis.

Drug content in release media was determined by high-performance liquid chromatography (HPLC) according to the United States Pharmacopeial (USP) method (United States Pharmacopeia and National Formulary (USP 34 – NF 29), 2011). The isocratic mobile phase was composed of solution A (15.2 mg/mL of triethylamine in water) at pH 3.0 adjusted with phosphoric acid, mixed to a 3:1 ratio with solution B (acetonitrile and 2-propanol, 3:2). A 50 μL injection volume and a Microsorb-MV C₁₈, 4.6 × 150 mm; 5 μm (Agilent Technologies) column were used. The isocratic separation was performed at a flow rate of 1 mL/min with UV detection at 220 nm. The retention time for LA was 5.5 – 6.5 min, followed by column washing with 80% methanol, 70% acetonitrile, and column re-equilibration with mobile phase.

For the 1-week *in vitro* drug release study, samples were prepared as described above, and analyzed according to Báez-Santos et al. (2016). In brief, aliquots of 200 μL were taken at 1, 6, and 24 h, and day 2, 3, 4, 5, and 7, followed by replacement of media with 200 μL of SBF. Time points were placed in 96-well black microplates and the concentration of LA in the release media was quantified by fluorescence spectroscopy using the Synergy™ H1 Multi-Mode Reader from BioTek®. The fluorescence intensities from released LA were measured using a gain of 78, monochromator bandwidth fixed at 16 nm, λ_{ex} = 280 nm, and λ_{em} = 340 nm. All measurements were taken within the assay's dynamic range.

3. Results and discussion

3.1. Phase behavior of the ternary phosphatidylcholine, sorbitan monooleate, and tocopherol acetate system

Phase behavior studies of the ternary PC, SMO, and TA (Fig. 1A) system were conducted to determine the lyotropic mesophases at 15 μL (13% (w/w)) and excess SBF to 100 μL of liquid crystal (LC) precursor. Initially, birefringence—a property of optically anisotropic samples such as hexagonal (H_{II}) or lamellar ($L\alpha$) mesophases (Rosevear, 1954)—was used for the qualitative assignment of isotropic and anisotropic phase regions. The phase diagram in Fig. 1B illustrates how isotropic solutions transition to anisotropic when PC is greater than 30% (w/w), SMO range from 10~75% (w/w), and TA range from 0~50% (w/w). The anisotropic phase region produced a range of morphologically different liquid crystalline materials with optically diverse birefringence patterns. Stronger birefringence patterns are observed at the center of the anisotropic phase region when the ratio of PC:SMO equals 1:1. The relative phase boundaries between the isotropic and anisotropic regions are illustrated in Fig. 1C.

Fig. 2A shows the plot of intensity versus the scattering vector, q , of representative H_{II} and $L\alpha$ mesophases formed by ternary PC, SMO, and TA samples in 13% (w/w) aqueous content. Within the anisotropic region of the phase diagram, well-separated and intense peaks in the SAXS diffraction patterns allowed for the assignment of mesophases corresponding to H_{II} and $L\alpha$ mesophases. At 13% (w/w) aqueous content (Fig. 2B), the majority of the anisotropic region corresponds to the $L\alpha$ mesophase. At high concentration of PC (50~60% (w/w)), a small region of H_{II} mesophase is present in formulations containing 20~40% (w/w) SMO and 0~20% (w/w) TA. As the PC concentration decreases below 50% (w/w), almost the entire phase diagram is essentially an oil-in-water emulsion and no other phases were detected.

Increasing the aqueous content resulted in a $L\alpha$ to H_{II} phase transition with a further region of H_{II} mesophases appearing at the lower PC concentration range of 40~50% (w/w), SMO from 40~75% (w/w), and TA from 0~50% (w/w) (Fig. 2C). Interestingly, at high aqueous content (from 31% (w/w) to excess) the SAXS scattering patterns revealed the presence of $L\alpha$ and H_{II} mixtures (Supplementary info), depending on the precise location where the

scattering profile was obtained from inside the capillary tube. Therefore, due to the transitional nature of the system at least three SAXS profiles were obtained from different locations in the capillary tube. Formulations with and without ethanol (no aqueous content) were also tested and no distinguishable phase was detected by SAXS.

3.2. In vitro release of leuprolide acetate from formulation candidates

The release of leuprolide acetate (LA) from this LC system was studied using eight selected formulations from the ternary phase diagram (Table 1) as a means to assess the individual excipient's impact on the release mechanism and kinetics. In addition, to further understand the impact of the mesophase on the release of LA, each formulation was evaluated as precursor oil versus their respective mesophase containing 13% (w/w) SBF. Due to the increase in LC matrix viscosity as a function of aqueous content, release studies from the mesophases was limited to those at 13% (w/w) SBF, where formulations still retain their syringeability.

Previous studies have reported that both the type and content of solvent can affect drug release from a liquid crystalline matrix (Ahmed et al., 2010; Chang and Bodmeier, 1998; Chen et al., 2015). A fixed solvent content of 10% (w/w) ethanol was used for all formulations to normalize any potential solvent effects (Ki et al., 2014). Fig. 3 illustrates the varying release profiles of LA from the different LC matrices. With the exception of F8, which lacks TA, all formulations displayed an overall slow release rate and less than 20% cumulative release at day 28 (Fig. 3A). Interestingly, the release from some partially preformed mesophases (Fig. 3B) was slightly greater relative to their precursor oils (Fig. 3A). This effect appears more prominent with increasing PC:SMO ratio, which includes F5, F6, F7, and F8 from the H_{II} mesophase.

A significant increase in drug release is observed with increasing PC:SMO ratio, with F7 providing the second most amount of LA release over 28 days. Furthermore, the complete removal of TA (F8) resulted in an additional ~60% increase in LA release. Unfortunately, additional formulations without TA tested that form an H_{II} mesophase required a larger amount of formulation vehicle to solubilize the LA and were excluded from further analysis. Nevertheless, it is evident from this data that the release rate for the binary system of PC and SMO (F8) is highly

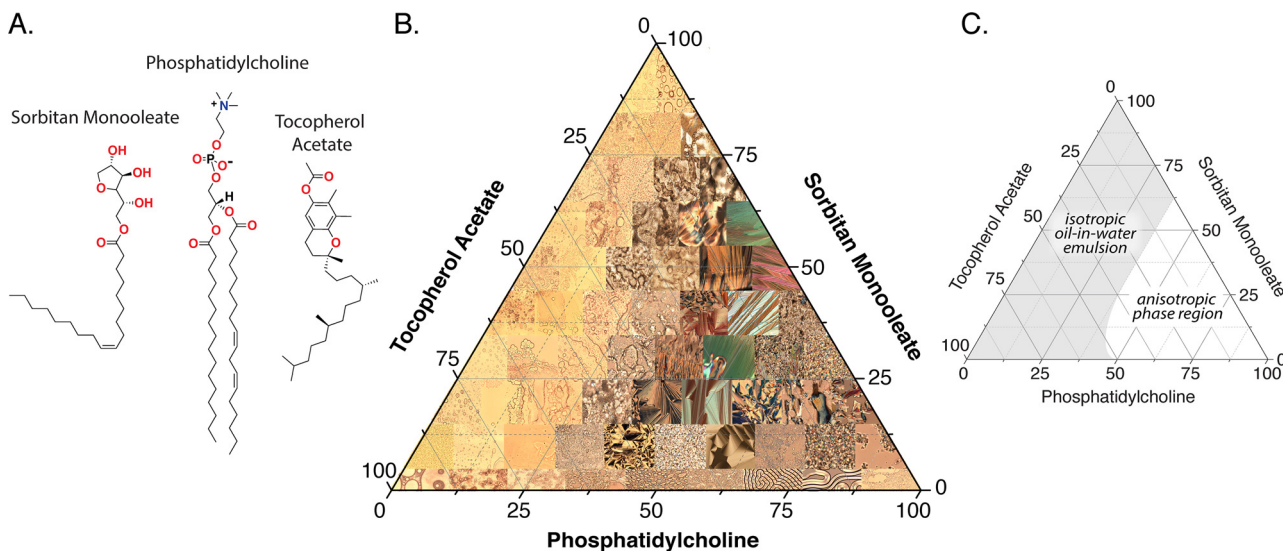


Fig. 1. Birefringence ternary phase diagram of SMO, PC, and TA. (A) Chemical structures of SMO, PC, and TA. (B) PLM images of each formulation across the phase diagram obtained in excess water where optical birefringence indicates the presence of the anisotropic H_{II} or $L\alpha$ mesophases. (C) Qualitative assignment of isotropic oil-in-water emulsion and anisotropic phase region based on PLM images in excess water.

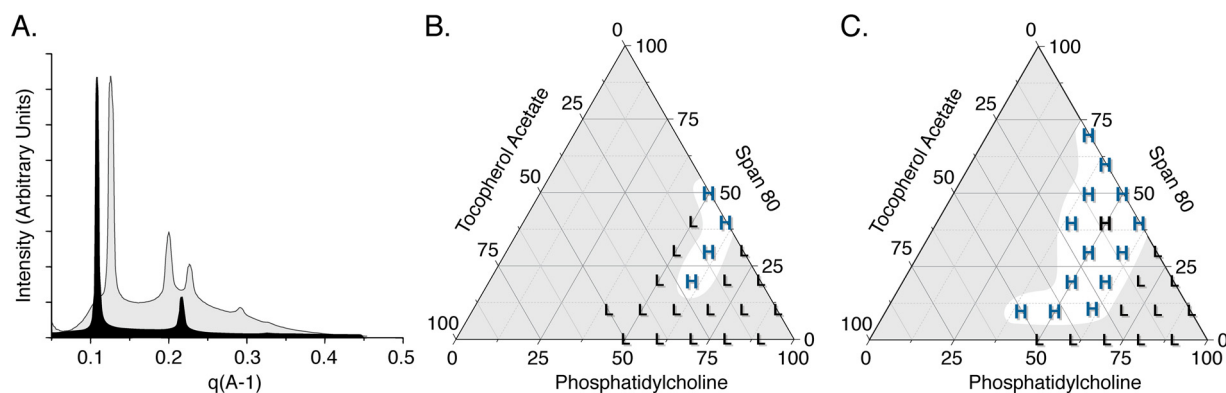


Fig. 2. Phase progression of the SMO, PC, and TA ternary system at fixed aqueous content. (A) SAXS patterns of selected $L\alpha$ (black) and H_{II} (gray) mesophases from the ternary mixtures of SMO, PC, and TA. Ternary phase diagrams by SAXS analysis at fixed aqueous content of 13% (w/w) (B) and excess (C). The zone of $L\alpha$ and H_{II} coexistence is highlighted in blue denoting the dominant mesophase.

Table 1

Composition of formulation candidates and their phase behavior.

Formulation	PC (%)	SMO (%)	TA (%)	Phase at 13% aqueous content	Phase at excess aqueous content
F1	40	10	50	$L\alpha$	$L\alpha$
F2	50	20	30	$L\alpha$	$H_{II}/L\alpha$
F3	50	30	20	$L\alpha$	$H_{II}/L\alpha$
F4	50	40	10	$L\alpha$	H_{II}
F5	60	10	30	$L\alpha$	$H_{II}/L\alpha$
F6	60	20	20	$H_{II}/L\alpha$	$H_{II}/L\alpha$
F7	60	30	10	$H_{II}/L\alpha$	$H_{II}/L\alpha$
F8	60	40	0	$H_{II}/L\alpha$	$H_{II}/L\alpha$

The quantities of PC, SMO, and TA are given as percentage by weight.

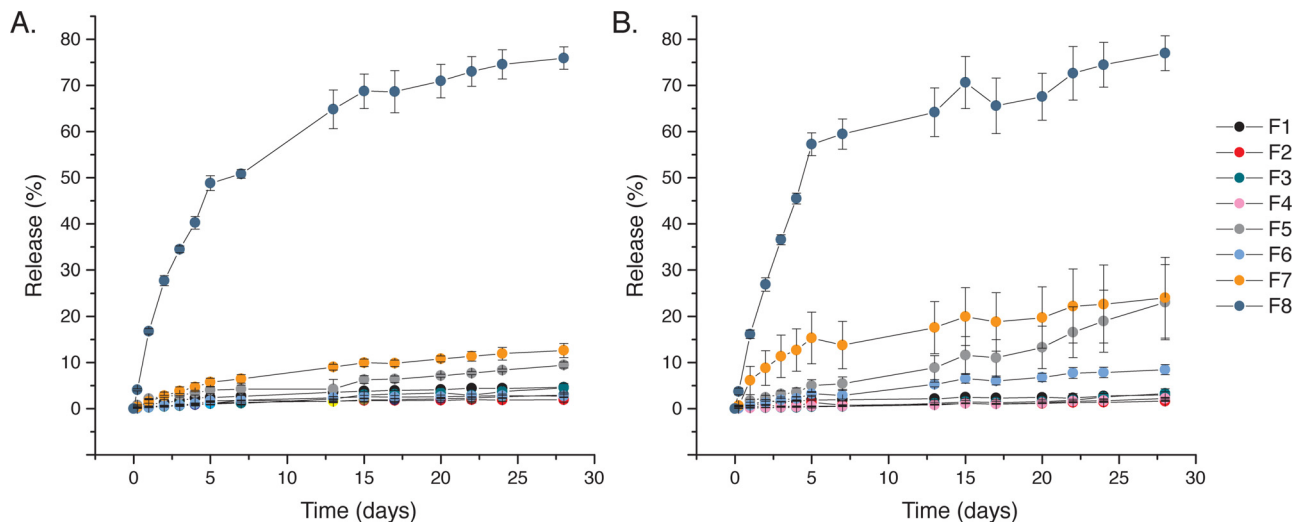


Fig. 3. Cumulative *in vitro* release of LA. The release profile from the precursor oils (A) versus their respective mesophases at 13% (w/w) aqueous content (B). Each point represents the mean \pm standard deviation of triplicate measurements.

divergent from the ternary system of PC, SMO, and TA. Therefore, it appears that TA plays a critical role in the release mechanism of LA.

3.3. Water uptake and erosion

The mechanism where TA leads to a decrease in LA release can be further explored by comparing the drug release to the water uptake properties of the formulations. The release profiles from partially pre-formed mesophases illustrated in Fig. 3B indicate a water-mediated mechanism of drug release taking place at an increasing PC:SMO ratio (F5–F8). This effect is further intensified

by the complete removal of TA (F8). Therefore, for the different formulations, the water uptake was monitored over time until equilibrium with water was reached, denoted as the water uptake capacity.

Equilibrium with water was reached at ~ 6 h, and all formulations were stable in equilibrium to the end of the study period (at least 14 days). Formulations F5, F6, F7, and F8 displayed a significant increase in both the rate of water uptake (Supplementary data) and water uptake capacity (Fig. 4). The water uptake capacity of the depot was very similar to that of the H_{II} + excess water boundary condition (Supplementary data), demonstrating

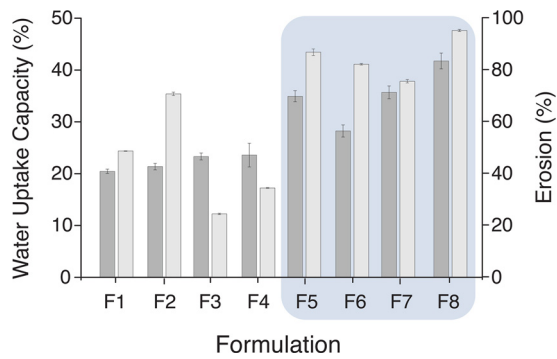


Fig. 4. Water uptake and erosion of formulation candidates. Water uptake capacity at equilibrium with water (dark gray, first y-axis) and percent erosion at 7 h endpoint (light gray, second y-axis). Highlighted in blue are formulations displaying superior water uptake capacity and erodability. Each point represents means \pm standard deviation of triplicate measurements.

that there appears to be a finite water swelling capacity for this system. Furthermore, the complete removal of TA (F8) resulted in an 8% increase in total water uptake. This further correlates with the 50~60% increase in total drug release relative to F7 (Fig. 3), suggesting TA has a mitigating effect on drug release by limiting the swelling capacity of the system.

The impact of TA on the release of LA is more evident for formulations containing less than 50% (w/w) PC, which could only reach ~20% total water uptake (Fig. 4) and resulted in less than ~10% release after 28 days (Fig. 3). Similarly to the swelling behavior, the erosion of the LC matrix in media containing 1% (v/v) Tween 20 (Fig. 4) was affected by the ternary component ratio, where 2 distinct groups of formulations emerged. Formulations with $\leq 50\%$ (w/w) PC had low to moderate water uptake and

erosion, whereas formulations containing 60% (w/w) PC had an increased water uptake capacity and erodability.

Chen et al. (2015), showed an increase in release rate with lowering water content (phytatriol-based system), whereas Chang and Bodmeier (1997a,b), showed an increase in release rate with increasing water content (monolinoleate system). While the LC systems, drug molecules, and LC structural pathways were different, the generalization of release patterns from LC systems seems to be case specific. For the system in question, a summary of the physicochemical parameters and LA release is shown in Fig. 5. The ternary-contour diagrams illustrate the influence the ternary component ratio has on the erodability, water uptake, and LA release. While their respective kinetics differ, partially due to experimental differences, the water uptake capacity highly correlates with the erodability of the formulation. Furthermore, these two characteristics appear to influence the amount of drug release, where drug release is favored by higher water content and erodability. Resistance to erosion in Tween 20 may indicate higher LC matrix strength, hence the low water uptake capacity and impaired drug release. Importantly, TA seems to play a role in mitigating the water absorption and erodability, ultimately decreasing the amount of drug release with increasing TA content.

To further understand the effect of the formulation on the microstructure, the lattice spacings were calculated for all the phases (Supplementary data). Similar to Phan et al. (2011), we found the lattice parameter cannot be used directly to correlate with the drug release behavior. In addition, since many of the phases in this study are mixtures of H_{II} & $L\alpha$, a relationship between the microstructure and release may be difficult to derive. Since the H_{II} is closed to the external environment (Boyd et al., 2006; Johnsson et al., 2005; Kaasgaard and Drummond, 2006; Sagalowicz et al., 2006), this phase may promote very slow release, overcoming the lower viscosities to that of the bicontinuous structures (Phan et al., 2011).

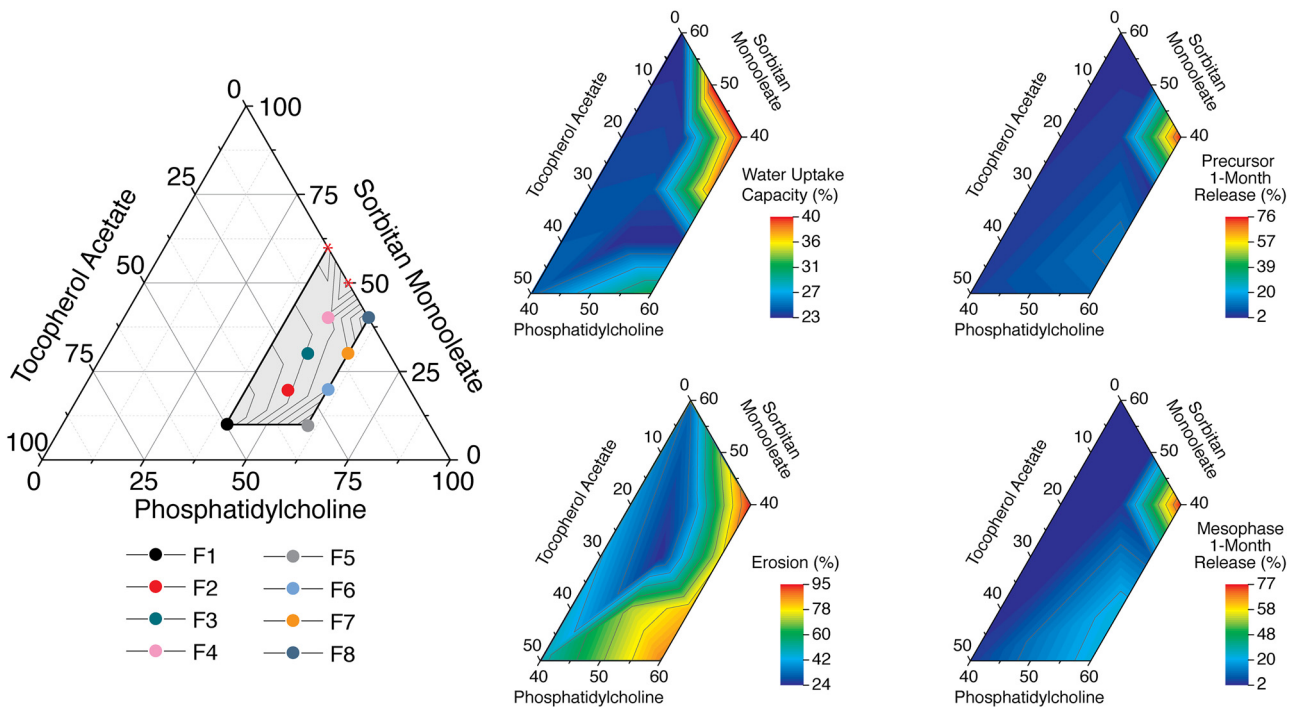


Fig. 5. Comparison of the physicochemical properties and drug release of formulation candidates. At the left-hand panel is the ternary diagram highlighting in gray the region of interest encompassing the ternary or binary composition of the formulation candidates (dots), and formulations that resulted in crystallization of LA and could not be used for drug release studies (red asterisk). The region of interest from the phase diagram is shown to the right as ternary-contour graphs, summarizing the physicochemical properties and drug release of the different formulations.

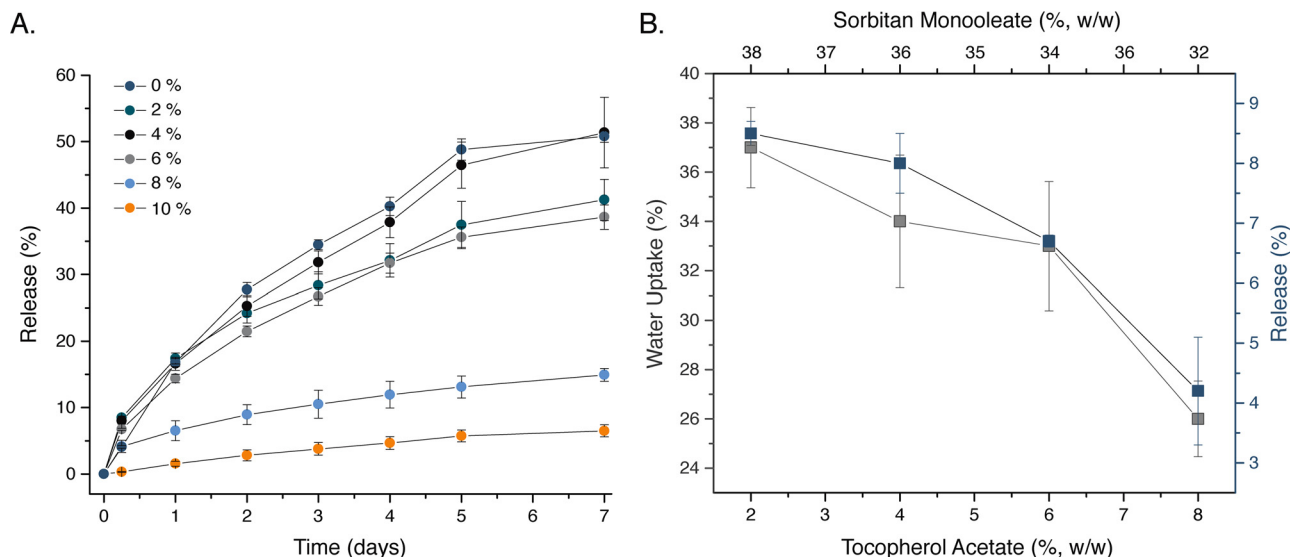


Fig. 6. Effect of TA on the *in vitro* release of LA and water uptake capacity of the LC. (A) One-week release profiles from formulations containing increments of 2% (w/w) TA between F7 (10%) and F8 (0%). (B) Comparison between total water uptake shown in gray (first y-axis) and LA release shown in blue (second y-axis) during the swelling period of 6 h. The excipients weight composition (% w/w) where PC is 60% is shown on first and second x-axes. Each point represents the mean \pm standard deviation of triplicate measurements.

3.4. Tocopherol acetate has a mitigating effect on the release of leuprolide acetate

Although the exact mechanism of LA release remains undetermined, our data indicates that TA plays a mitigating role on the release of LA. Considering the structural attributes of the H_{II} mesophase, one can assume that the aqueous water channels are closed extended micellar columnar structures (Boyd et al., 2006; Johnson et al., 2005; Kaasgaard and Drummond, 2006; Sagalowitz et al., 2006). Therefore, hydrophilic molecules, LA in particular based on its hydrophilicity and large size, relative to a small molecule, would most likely require random perturbations and/or dynamic deconstruction/reconstruction events of the reverse micelles to provide drug release once “trapped” inside the shell of the H_{II} mesophase. At 28 days, drug release of >10% is only observed for two of the formulations, F7 and F8, further alluding to the closed channels. It is hypothesized that TA may act as a perturbation inhibitor in the PC and SMO lipid chains, resulting in slower diffusion of LA from the mesophase. The position of TA in phospholipid bilayers has been previously suggested to be in the hydrophobic domain of the phospholipid chains (Massey, 2001; Villalain et al., 1986). Based on this data and previous reports, release experiments from formulations containing increments of 2% (w/w) TA between F7 and F8 were performed as a means to further characterize the functionality of TA in this system.

The 1-week *in vitro* release study resulted in similar amounts of LA release (40–50%) from formulations comprised of 2–6% (w/w) TA (Fig. 6A), and were not significantly different to F8 containing 0% TA. At 8% (w/w) TA, a significant decrease from ~50% to ~14% LA release was observed, also approaching F7 (10% (w/w) TA) which resulted in an overall LA release of 7%. Analysis of water uptake during the first 6 h of swelling resulted in similar trends (Fig. 6B), with ~10% decreased water absorption at 8% (w/w) TA. Thus, 8% (w/w) TA was established as the minimum concentration threshold for the divergence of release profiles.

4. Conclusions

Several potential advantages can be concluded about this LC system. First, the high similarity between the release patterns of

the precursor oil and pre-formed mesophase formulations enables the further development of subcutaneous injections using the low viscosity precursor oil formulations. Second, the characterization of physicochemical properties and drug release across the phase diagram revealed a crucial role for TA. In understanding the mechanism of drug release, a link between water uptake, erodability, and LA release was determined. TA plays a major role in mitigating drug release by altering the physicochemical properties of the LC matrix. Formulations with low amounts of TA and higher water uptake capacities were found to have a higher propensity towards erodability, a potential clue to its *in vivo* biodegradability. More importantly, the high impact of TA on the release of LA indicates the use of TA as a tailoring agent for this LC system, broadening the therapeutic applications to other active pharmaceutical ingredients.

Acknowledgments

This research was supported by Chong Kun Dang Pharmaceutical Corp. We thank the beamline scientists at 12-BM-B at the Advanced Photon Source, an Office of Science User Facility operated for the U.S. Department of Energy (DOE) Office of Science by Argonne National Laboratory, which is supported by the U.S. DOE under Contract No. DE-AC02-06CH11357.

Appendix A. Supplementary data

Supplementary data associated with this article can be found, in the online version, at <http://dx.doi.org/10.1016/j.ijpharm.2016.06.138>.

References

- Ahmed, A.R., Dashevsky, A., Bodmeier, R., 2010. Drug release from and sterilization of *in situ* cubic phase forming monoglyceride drug delivery systems. *Eur. J. Pharm. Biopharm.* 75, 375–380. doi:<http://dx.doi.org/10.1016/j.ejpb.2010.04.004>.
- Angelico, R., Ceglie, A., Olsson, U., Palazzo, G., 2000. Phase diagram and phase properties of the system lecithin-Water-Cyclohexane. *Langmuir* 16, 2124–2132. doi:<http://dx.doi.org/10.1021/la9909190>.
- Angelova, A., Angelov, B., Mutafchieva, R., Lesieur, S., Couvreur, P., 2011. Self-assembled multicompartiment liquid crystalline lipid carriers for protein,

- peptide, and nucleic acid drug delivery. *Acc. Chem. Res.* 44, 147–156. doi:http://dx.doi.org/10.1021/ar100120v.
- Báez-Santos, Y.M., Ottea, A., Park, K., 2016. A fast and sensitive method for the detection of leuprolide acetate: a high-throughput approach for the in vitro evaluation of liquid crystal formulations. *Anal. Chem.* doi:http://dx.doi.org/10.1021/acs.analchem.6b00190.
- Barauskas, J., Landh, T., 2003. Phase behavior of the Phytantriol/Water system. *Langmuir* 19, 9562–9565.
- Boyd, B.J., Whittaker, D.V., Khoo, S.-M., Davey, G., 2006. Lyotropic liquid crystalline phases formed from glycerate surfactants as sustained release drug delivery systems. *Int. J. Pharm.* 309, 218–226. doi:http://dx.doi.org/10.1016/j.ijpharm.2005.11.033.
- Boyd, B.J., 2003. Characterisation of drug release from cubosomes using the pressure ultrafiltration method. *Int. J. Pharm.* 260, 239–247. doi:http://dx.doi.org/10.1016/S0378-5173(03)00262-X.
- Cervin, C., Vandoolaeghe, P., Nistor, C., Tiberg, F., Johnsson, M., 2009. A combined in vitro and in vivo study on the interactions between somatostatin and lipid-based liquid crystalline drug carriers and bilayers. *Eur. J. Pharm. Sci.* 36, 377–385. doi:http://dx.doi.org/10.1016/j.ejps.2008.11.001.
- Cervin, C., Tinzl, M., Johnsson, M., Abrahamsson, P.A., Tiberg, F., Dizayi, N., 2010. Properties and effects of a novel liquid crystal nanoparticle formulation of docetaxel in a prostate cancer mouse model. *Eur. J. Pharm. Sci.* 41, 369–375. doi:http://dx.doi.org/10.1016/j.ejps.2010.07.003.
- Chang, C.M., Bodmeier, R., 1997a. Binding of drugs to monoglyceride-based drug delivery systems. *Int. J. Pharm.* 147, 135–142. doi:http://dx.doi.org/10.1016/S0378-5173(96)04805-3.
- Chang, C.M., Bodmeier, R., 1997b. Swelling of and drug release from monoglyceride-Based drug delivery systems. *J. Pharm. Sci.* 86, 747–752.
- Chang, C.M., Bodmeier, R., 1998. Low viscosity monoglyceride-based drug delivery systems transforming into a highly viscous cubic phase. *Int. J. Pharm.* 173, 51–60. doi:http://dx.doi.org/10.1016/S0378-5173(98)00180-X.
- Chen, Y., Ma, P., Gui, S., 2014. Cubic and hexagonal liquid crystals as drug delivery systems. *Biomed Res. Int.* 2014, 1–12. doi:http://dx.doi.org/10.1155/2014/815981.
- Chen, Y., Liang, X., Ma, P., Tao, Y., Wu, X., Wu, X., Chu, X., Gui, S., 2015. Phytantriol-Based In situ liquid crystals with long-Term release for intra-articular administration. *AAPS PharmSciTech* 16, 846–854. doi:http://dx.doi.org/10.1208/s12249-014-0277-6.
- Clagston, J., Caffrey, M., 2005. Controlling release from the lipidic cubic phase Amino acids, peptides, proteins and nucleic acids. *J. Control. Release* 107, 97–111. doi:http://dx.doi.org/10.1016/j.jconrel.2005.05.015.
- Drummond, C.J., Fong, C., 1999. Surfactant self-assembly objects as novel drug delivery vehicles. *Curr. Opin. Colloid Interface Sci.* doi:http://dx.doi.org/10.1016/S1359-0294(00)00020-0.
- Guo, C., Wang, J., Cao, F., Lee, R.J., Zhai, G., 2010. Lyotropic liquid crystal systems in drug delivery. *Drug Discov. Today* 15, 1032–1040. doi:http://dx.doi.org/10.1016/j.drudis.2010.09.006.
- Hiltrop, K., 1994. In: Stegemeyer, H., Behret, H. (Eds.), *Liquid Crystals*. Steinkopff, Heidelberg, pp. 143–171. doi:http://dx.doi.org/10.1007/978-3-662-08393-2_4.
- Huang, T.C., Toraya, H., Blanton, T.N., Wu, Y., 1993. X-ray powder diffraction analysis of silver behenate, a possible low-angle diffraction standard. *J. Appl. Crystallogr.* 26, 180–184. doi:http://dx.doi.org/10.1107/S0021889892009762.
- Hyde, S., Ninham, B.W., Andersson, S., Larsson, K., Landh, T., Blum, Z., Lidin, S., 1997. The language of shape. *The Language of Shape*. Elsevier doi:http://dx.doi.org/10.1016/B978-044481538-5/50004-6.
- Ilavsky, J., 2012. Nika: software for two-dimensional data reduction. *J. Appl. Crystallogr.* 45, 324–328. doi:http://dx.doi.org/10.1107/S0021889812004037.
- Johnsson, M., Lam, Y., Barauskas, J., Tiberg, F., 2005. Aqueous phase behavior and dispersed nanoparticles of diglycerol monooleate/glycerol dioleate mixtures. *Langmuir* 21, 5159–5165. doi:http://dx.doi.org/10.1021/la050175s.
- Johnsson, M., Barauskas, J., Norlin, A., Tiberg, F., 2006. Physicochemical and drug delivery aspects of lipid-based liquid crystalline nanoparticles: a case study of intravenously administered propofol. *J. Nanosci. Nanotechnol.* 6, 3017–3024. doi:http://dx.doi.org/10.1166/jnn.2006.402.
- Kaasgaard, T., Drummond, C.J., 2006. Ordered 2-D and 3-D nanostructured amphiphile self-assembly materials stable in excess solvent. *Phys. Chem. Chem. Phys.* 8, 4957–4975. doi:http://dx.doi.org/10.1039/b609510k.
- Ki, M.-H., Lim, J.-L., Ko, J.-Y., Park, S.-H., Kim, J.-E., Cho, H.-J., Park, E.-S., Kim, D.-D., 2014. A new injectable liquid crystal system for one month delivery of leuprolide. *J. Control. Release* 185, 62–70. doi:http://dx.doi.org/10.1016/j.jconrel.2014.04.034.
- Lopes, L.B., Lopes, J.L.C., Oliveira, D.C.R., Thomazini, J.A., Garcia, M.T.J., Fantini, M.C.A., Collett, J.H., Bentley, M.V.L.B., 2006. Liquid crystalline phases of monoolein and water for topical delivery of cyclosporin A: Characterization and study of in vitro and in vivo delivery. *Eur. J. Pharm. Biopharm.* 63, 146–155. doi:http://dx.doi.org/10.1016/j.ejpb.2006.02.003.
- Luzzati, V., Husson, F., 1962. The structure of the liquid crystalline phases of lipid-water systems. *J. Cell Biol.* 12, 207–219.
- Marques, M.R.C., Loebenberg, R., Almkainzi, M., 2011. Simulated biological fluids with possible application in dissolution testing. *Dissolution Technol.* 10, 1002/jps 23029.
- Martiel, I., Sagalowicz, L., Mezzenga, R., 2014. Phospholipid-based nonlamellar mesophases for delivery systems: bridging the gap between empirical and rational design. *Adv. Colloid Interface Sci.* doi:http://dx.doi.org/10.1016/j.cis.2014.03.005.
- Martiel, I., Baumann, N., Vallooran, J.J., Bergfreund, J., Sagalowicz, L., Mezzenga, R., 2015. Oil and drug control the release rate from lyotropic liquid crystals. *J. Control. Release* 204, 78–84. doi:http://dx.doi.org/10.1016/j.jconrel.2015.02.034.
- Massey, J.B., 2001. Interfacial properties of phosphatidylcholine bilayers containing vitamin E derivatives. *Chem. Phys. Lipids* 109, 157–174. doi:http://dx.doi.org/10.1016/S0009-3084(00)00216-4.
- Negrini, R., Mezzenga, R., 2011. pH-responsive lyotropic liquid crystals for controlled drug delivery. *Langmuir* 3393, 5296–5303.
- Nguyen, T.-H., Hanley, T., Porter, C.J.H., Larson, I., Boyd, B.J., 2010. Phytantriol and glyceryl monooleate cubic liquid crystalline phases as sustained-release oral drug delivery systems for poorly water-soluble drugs II. In-vivo evaluation. *J. Pharm. Pharmacol.* 62, 856–865. doi:http://dx.doi.org/10.1211/jpp.62.06.0006 ([PMP1103]pii).
- Nielsen, L.S., Schubert, L., Hansen, J., 1998. Bioadhesive drug delivery systems. I. Characterisation of mucoadhesive properties of systems based on glyceryl mono-oleate and glyceryl monolinoleate. *Eur. J. Pharm. Sci.* 6, 231–239. doi:http://dx.doi.org/10.1016/S0928-0987(97)10004-5.
- Phan, S., Fong, W.K., Kirby, N., Hanley, T., Boyd, B.J., 2011. Evaluating the link between self-assembled mesophase structure and drug release. *Int. J. Pharm.* 421, 176–182. doi:http://dx.doi.org/10.1016/j.ijpharm.2011.09.022.
- Phelps, J., Bentley, M.V.L.B., Lopes, L.B., 2011. In situ gelling hexagonal phases for sustained release of an anti-addiction drug. *Colloids Surf. B Biointerfaces* 87, 391–398. doi:http://dx.doi.org/10.1016/j.colsurfb.2011.05.048.
- Qiu, H., Caffrey, M., 1998. Lyotropic and thermotropic phase behavior of hydrated monoacylglycerols: structure characterization of monovaccenin †. *J. Phys. Chem. B* 102, 4819–4829. doi:http://dx.doi.org/10.1021/jp980553k.
- Rosevear, F.B., 1954. The microscopy of the liquid crystalline neat and middle phases of soaps and synthetic detergents. *J. Am. Oil Chem. Soc.* 31, 628–639. doi:http://dx.doi.org/10.1007/BF02545595.
- Sagalowicz, L., Mezzenga, R., Leser, M.E., 2006. Investigating reversed liquid crystalline mesophases. *Curr. Opin. Colloid Interface Sci.* 11, 224–229. doi:http://dx.doi.org/10.1016/j.cocis.2006.07.002.
- Sagalowicz, L., Guillot, S., Acquistapace, S., Schmitt, B., Maurer, M., Yaghmur, A., De Campo, L., Rouvet, M., Leser, M., Glatter, O., 2013. Influence of vitamin E acetate and other lipids on the phase behavior of mesophases based on unsaturated monoglycerides. *Langmuir* 29, 8222–8232. doi:http://dx.doi.org/10.1021/la305052q.
- Seddon, J.M., 1990. Structure of the inverted hexagonal (HII) phase, and non-lamellar phase transitions of lipids. *Biochim. Biophys. Acta* 1031, 1–69. doi:http://dx.doi.org/10.1016/0304-4157(90)90002-T.
- Shah, J.C., Sadhale, Y., Chilukuri, D.M., 2001. Cubic phase gels as drug delivery systems. *Adv. Drug Deliv. Rev.* 47, 229–250. doi:http://dx.doi.org/10.1016/S0169-409X(01)00108-9.
- Tiberg, F., Johnsson, M., 2011. Drug delivery applications of non-lamellar liquid crystalline phases and nanoparticles. *J. Drug Deliv. Sci. Technol.* 21, 101–109. doi:http://dx.doi.org/10.1016/S1773-2247(11)50009-7.
- Tiberg, F., Roberts, J., Cervin, C., Johnsson, M., Sarp, S., Tripathi, A.P., Linden, M., 2015. Octreotide s.c. depot provides sustained octreotide bioavailability and similar IGF-1 suppression to octreotide LAR in healthy volunteers. *Br. J. Clin. Pharmacol.* doi:http://dx.doi.org/10.1111/bcp.12698.
- United States Pharmacopeia and National Formulary (USP 34 – NF 29), 2011.**
- Villalain, J., Aranda, F.J., Gómez-Fernández, J.C., 1986. Calorimetric and infrared spectroscopic studies of the interaction of alpha-tocopherol and alpha-tocopheryl acetate with phospholipid vesicles. *Eur. J. Biochem.* 158, 141–147. doi:http://dx.doi.org/10.1111/j.1432-1033.1986.tb09731.x.
- Yaghmur, A., Laggner, P., Almgren, M., Rappolt, M., 2008. Self-assembly in monoolein aqueous dispersions: direct vesicles to cubosomes transition. *PLoS One* 3, 42–46. doi:http://dx.doi.org/10.1371/journal.pone.0003747.
- Zabara, A., Mezzenga, R., 2014. Controlling molecular transport and sustained drug release in lipid-based liquid crystalline mesophases. *J. Control. Release* 188, 31–43. doi:http://dx.doi.org/10.1016/j.jconrel.2014.05.052.